



**Defense Threat Reduction Agency  
8725 John J. Kingman Road, MS-6201  
Fort Belvoir, VA 22060-6201**



**DTRA-TR-16-054**

# TECHNICAL REPORT

## **Approximating the Probability of Mortality Due To Protracted Radiation Exposures**

DISTRIBUTION A. Approved for public release: distribution is unlimited.

June 2016

HDTRA1-14-D-0003; 0005

Prepared by:

Applied Research Associates, Inc.  
801 N. Quincy Street  
Suite 700  
Arlington, VA 22203

This page intentionally left blank.

<b>REPORT DOCUMENTATION PAGE</b>					<i>Form Approved OMB No. 0704-0188</i>	
<small>The public reporting burden for this collection of information is estimated to average 1 hour per response, including the time for reviewing instructions, searching existing data sources, gathering and maintaining the data needed, and completing and reviewing the collection of information. Send comments regarding this burden estimate or any other aspect of this collection of information, including suggestions for reducing the burden, to Department of Defense, Washington Headquarters Services, Directorate for Information Operations and Reports (0704-0188), 1215 Jefferson Davis Highway, Suite 1204, Arlington, VA 22202-4302. Respondents should be aware that notwithstanding any other provision of law, no person shall be subject to any penalty for failing to comply with a collection of information if it does not display a currently valid OMB control number.</small>						
<b>PLEASE DO NOT RETURN YOUR FORM TO THE ABOVE ADDRESS.</b>						
<b>1. REPORT DATE (DD-MM-YYYY)</b>		<b>2. REPORT TYPE</b>			<b>3. DATES COVERED (From - To)</b>	
<b>4. TITLE AND SUBTITLE</b>				<b>5a. CONTRACT NUMBER</b>		
				<b>5b. GRANT NUMBER</b>		
				<b>5c. PROGRAM ELEMENT NUMBER</b>		
<b>6. AUTHOR(S)</b>				<b>5d. PROJECT NUMBER</b>		
				<b>5e. TASK NUMBER</b>		
				<b>5f. WORK UNIT NUMBER</b>		
<b>7. PERFORMING ORGANIZATION NAME(S) AND ADDRESS(ES)</b>					<b>8. PERFORMING ORGANIZATION REPORT NUMBER</b>	
<b>9. SPONSORING/MONITORING AGENCY NAME(S) AND ADDRESS(ES)</b>					<b>10. SPONSOR/MONITOR'S ACRONYM(S)</b>	
					<b>11. SPONSOR/MONITOR'S REPORT NUMBER(S)</b>	
<b>12. DISTRIBUTION/AVAILABILITY STATEMENT</b>						
<b>13. SUPPLEMENTARY NOTES</b>						
<b>14. ABSTRACT</b>						
<b>15. SUBJECT TERMS</b>						
<b>16. SECURITY CLASSIFICATION OF:</b>			<b>17. LIMITATION OF ABSTRACT</b>	<b>18. NUMBER OF PAGES</b>	<b>19a. NAME OF RESPONSIBLE PERSON</b>	
a. REPORT	b. ABSTRACT	c. THIS PAGE			<b>19b. TELEPHONE NUMBER (Include area code)</b>	

## UNIT CONVERSION TABLE

U.S. customary units to and from international units of measurement<sup>\*</sup>

U.S. Customary Units	<div style="display: flex; align-items: center; justify-content: center;"> <div style="margin-right: 10px;"> </div> Multiply by </div> <div style="display: flex; align-items: center; justify-content: center;"> <div style="margin-right: 10px;"> </div> Divide by<sup>†</sup> </div>	International Units
<b>Length/Area/Volume</b>		
inch (in)	2.54 × 10 <sup>-2</sup>	meter (m)
foot (ft)	3.048 × 10 <sup>-1</sup>	meter (m)
yard (yd)	9.144 × 10 <sup>-1</sup>	meter (m)
mile (mi, international)	1.609 344 × 10 <sup>3</sup>	meter (m)
mile (nmi, nautical, U.S.)	1.852 × 10 <sup>3</sup>	meter (m)
barn (b)	1 × 10 <sup>-28</sup>	square meter (m <sup>2</sup> )
gallon (gal, U.S. liquid)	3.785 412 × 10 <sup>-3</sup>	cubic meter (m <sup>3</sup> )
cubic foot (ft <sup>3</sup> )	2.831 685 × 10 <sup>-2</sup>	cubic meter (m <sup>3</sup> )
<b>Mass/Density</b>		
pound (lb)	4.535 924 × 10 <sup>-1</sup>	kilogram (kg)
unified atomic mass unit (amu)	1.660 539 × 10 <sup>-27</sup>	kilogram (kg)
pound-mass per cubic foot (lb ft <sup>-3</sup> )	1.601 846 × 10 <sup>1</sup>	kilogram per cubic meter (kg m <sup>-3</sup> )
pound-force (lbf avoirdupois)	4.448 222	newton (N)
<b>Energy/Work/Power</b>		
electron volt (eV)	1.602 177 × 10 <sup>-19</sup>	joule (J)
erg	1 × 10 <sup>-7</sup>	joule (J)
kiloton (kt) (TNT equivalent)	4.184 × 10 <sup>12</sup>	joule (J)
British thermal unit (Btu) (thermochemical)	1.054 350 × 10 <sup>3</sup>	joule (J)
foot-pound-force (ft lbf)	1.355 818	joule (J)
calorie (cal) (thermochemical)	4.184	joule (J)
<b>Pressure</b>		
atmosphere (atm)	1.013 250 × 10 <sup>5</sup>	pascal (Pa)
pound force per square inch (psi)	6.984 757 × 10 <sup>3</sup>	pascal (Pa)
<b>Temperature</b>		
degree Fahrenheit (°F)	[T(°F) – 32]/1.8	degree Celsius (°C)
degree Fahrenheit (°F)	[T(°F) + 459.67]/1.8	kelvin (K)
<b>Radiation</b>		
curie (Ci) [activity of radionuclides]	3.7 × 10 <sup>10</sup>	per second (s <sup>-1</sup> ) [becquerel (Bq)]
roentgen (R) [air exposure]	2.579 760 × 10 <sup>-4</sup>	coulomb per kilogram (C kg <sup>-1</sup> )
rad [absorbed dose]	1 × 10 <sup>-2</sup>	joule per kilogram (J kg <sup>-1</sup> ) [gray (Gy)]
rem [equivalent and effective dose]	1 × 10 <sup>-2</sup>	joule per kilogram (J kg <sup>-1</sup> ) [sievert (Sv)]

<sup>\*</sup>Specific details regarding the implementation of SI units may be viewed at <http://www.bipm.org/en/si/>.

<sup>†</sup>Multiply the U.S. customary unit by the factor to get the international unit. Divide the international unit by the factor to get the U.S. customary unit.

## Table of Contents

Table of Contents .....	i
List of Figures .....	ii
List of Tables .....	iii
Acknowledgements .....	iv
Abstract .....	1
Section 1. Introduction .....	2
Section 2. The MARCELL Model for Radiation-Induced Mortality .....	3
Section 3. Prompt Dose Mortality .....	4
Section 4. Exposure at Constant Dose Rate .....	5
Section 5. Dose-Response Approximations for Exposure at Constant Dose Rate .....	10
Section 6. Exposure in a Nuclear Fallout Field .....	15
Section 7. Dose-Response Approximation for Exposure in a Fallout Field .....	18
Section 8. Conclusion .....	21
Section 9. References .....	22

## List of Figures

Figure 1. The prompt dose mortality curve used in RIPD has a steeper slope than that of the older CHRNEM software. ....	4
Figure 2. Because of biological repair and recovery processes, the median lethal dose for exposures at a constant dose rate increases with increasing duration of exposure.....	6
Figure 3. Data from Figure 2 plotted with a logarithmic time scale.....	7
Figure 4. Median lethal dose for exposures at constant dose rate plotted as a function of dose rate (exposure duration is determined by dose rate, because biological effect is fixed).....	8
Figure 5. The EPD for a 410 cGy dose delivered at constant dose rate also has a power behavior over a limited range of dose rates. ....	9
Figure 6. Response parameters for constant dose rate exposure. ....	10
Figure 7. Curve shows sixth-order polynomial fit to the LD <sub>50</sub> data (circles) from Table 1. Coefficients of the polynomial are listed in Table 2.....	12
Figure 8. Curve shows sixth-order polynomial fit to the LD <sub>10</sub> data (circles) from Table 1. Coefficients of the polynomial are listed in Table 2.....	12
Figure 9. Curve shows sixth-order polynomial fit to the LD <sub>90</sub> data (circles) from Table 1. Coefficients of the polynomial are listed in Table 2.....	13
Figure 10. With fallout age fixed at 1 h, the median lethal dose as a function of exposure duration is similar to that for a constant dose rate exposure when the exposure duration is less than four days. ....	16
Figure 11. The median lethal dose for a 48 h exposure in a fallout field depends on the age of the fallout at the time of entry into the fallout field.....	17
Figure 12. The rule of thumb gives an LD <sub>50</sub> of about 640 cGy (circled point) for a 48 h exposure, in quite good agreement with the fallout calculation from RIPD for a fallout age at entry of 0.3 h. ....	19
Figure 13. HPAC comparison of 48-hour integrated dose from fallout and the resulting probability of fatality shows the reduction in mortality caused by dose protraction for a 10 KT ground burst. (Note that the probability of fatality includes prompt weapon effects while the integrated dose does not.).....	21

## List of Tables

Table 1. Data from Figure 6 showing the relatively small variation in the slope of the dose response curve as measured by the ratio of the LD <sub>90</sub> to the LD <sub>10</sub> . .....	11
Table 2. Coefficients for sixth-order polynomial fits to the data in Table 1. Independent variable is $\log_{10}(\text{time in hours})$ . Polynomial gives $\log_{10}(\text{dose in cGy})$ . .....	13
Table 3. Rule of thumb provides results intermediate to fallout ages of 0.2 and 1.0 h. ....	19

## **Acknowledgements**

This work was originally performed as part of the CBRNE Risk Assessment for Human Response and Health Effects contract, DTRA-01-03-D-0014-0015, under Mr. Eric Nelson at NTMP. That contract included a wide-range of tasks designed to support the Hazard Prediction and Assessment Capability (HPAC) and NBC Casualty and Resource Estimation Support Tool (NBC CREST).

Under the current Nuclear Survivability and Forensics contract, HDTRA1-14-D-0003; 0005, Dr. Paul Blake of DTRA/NTPR has supported the transition of this work into a technical report so that results based on the methodologies described here can be accessed.



## **Abstract**

Probability of fatality plots in HPAC for whole body exposure due to nuclear weapons frequently indicate a median lethal dose ( $LD_{50}$ ) much higher than the prompt dose value, even for acute exposures. This apparent paradox is discussed in this paper. We conclude that the values generated by HPAC are reasonable in the MARCELL model, which includes the effects of bone marrow cell damage, repair and death. Values of fallout age-at-entry and exposure duration encountered in HPAC calculations typically generate exposures having  $LD_{50}$  ranging from 600 to 700 cGy, instead of the prompt value of 410 cGy. We present approximate methods for estimating the probability of mortality due to radiological environments from nuclear weapon detonations or from a radiological dispersal device.

## **Section 1.**

### **Introduction**

In the Hazard Prediction and Assessment Capability (HPAC) software, probability of mortality for whole-body, protracted radiation exposure in the fallout field of a nuclear detonation is based on the Radiation-Induced Performance Decrement (RIPD) software developed by the Defense Nuclear Agency in the 1990s. The purpose of this paper is to better explain the qualitative and quantitative features of mortality due to protracted radiation exposure and to show how characteristic values for median lethal dose from fallout exposure arise in HPAC calculations.

A sometimes puzzling feature of the probability of mortality contours generated by HPAC for nuclear fallout is the occurrence of median lethal dose ( $LD_{50}$ ) values between 600 and 700 cGy, significantly higher than the prompt dose value of 410 cGy. The puzzle is exacerbated when exposure durations of 24 or 48 hours are referred to as “acute” doses, implying that they ought to have an  $LD_{50}$  near that of a prompt dose. Biologically, prompt doses delivered in less than a minute have a significantly different effect than those delivered over periods lasting an hour or longer. The data and discussions below provide illustrations of this difference and some insight into the occurrence of  $LD_{50}$  values around 700 cGy.

Because the RIPD code is computationally intensive, it is useful to have an easier, approximate calculation for estimating probability of mortality due to protracted radiation exposure. The following discussion provides an overview of RIPD calculations for selected exposure histories and presents approximations that may be used for a range of situations related to nuclear fallout and other radiological exposures.

## Section 2.

### The MARCELL Model for Radiation-Induced Mortality

The probability of mortality in RIPD is calculated with the marrow cell (MARCELL) model (Jones *et al.*, 1993b) developed at Oak Ridge National Laboratory (ORNL) for the Defense Nuclear Agency. The model estimates mortality due to the hematopoietic syndrome of acute radiation sickness. In the MARCELL model, radiation exposure dynamically depletes the bone marrow cell population, the underpinning of the immune system. For any protracted exposure, an equivalent prompt dose (EPD) is estimated by finding the prompt dose that produces the same marrow cell population nadir (maximum cytopenia) as the protracted dose in question. This EPD is used in conjunction with a lognormal, dose-response curve for prompt doses to determine the probability of mortality for the protracted exposure.

MARCELL is a physiologically based, cell-kinetics model of the response of bone marrow tissue to radiation exposure (see the Appendix of Jones *et al.*, 1994a for a description of the model and equations). The model tracks the marrow cell population in three compartments: normal, injured, and killed cells. The compartment populations are described by a set of differential (rate) equations emulating normal cell turnover, radiation damage, repair of damage, cell killing, and tissue recovery. At zero dose rate, the set of equations has an equilibrium solution corresponding to a healthy individual. The equations contain the radiation dose rate as a driving term that creates cell damage, thereby depleting the marrow cell population. The cell population recovers either after the exposure ends or when the dose rate drops below a level where cell proliferation can compensate for the continuing cell depletion rate. Depletion resumes if the dose rate is increased again. This modeling approach accommodates temporally varying dose rates including combinations of prompt and fallout radiation exposures. The RIPD software numerically solves the MARCELL model equations for an exposure history defined by the user.

The development, testing, and application of the MARCELL model is extensively documented in a series of journal publications sponsored by the Defense Nuclear Agency (Jones *et al.* and Morris *et al.*, 1991-1997). In these references, the MARCELL model is applied to both data from animal experiments and data from relevant human sources. Animal experiments on a wide variety of species validate the way in which MARCELL models the effects of dose protraction on mortality. Parameters built into RIPD are the best available set for estimating human mortality (see Table 4 of Jones *et al.*, 1994a). The RIPD implementation of the MARCELL model has been verified against results published by the ORNL group (Morris *et al.*, 1994) and those calculated with an ORNL software version of the model named MarCel21.

## Section 3.

### Prompt Dose Mortality

The probability of mortality calculation in RIPD and RIPDLPI (Radiation-Induced Performance Decrement Lethality Injury Probability Interpolation) is referenced to a lognormal dose-response curve for prompt doses (Anno *et al.*, 2003) having a median lethal dose ( $LD_{50}$ ) of 410 cGy free-in-air (FIA) tissue kerma and a (probit) slope of 7.1 (using base-10 logarithms). Figure 1 compares this prompt dose-response curve with that used in the Combined Human Response Nuclear Effects Model (CHRNEM), which is based on the same  $LD_{50}$  value but a shallower slope of 4.4 (Levin and Fulton, 1992).

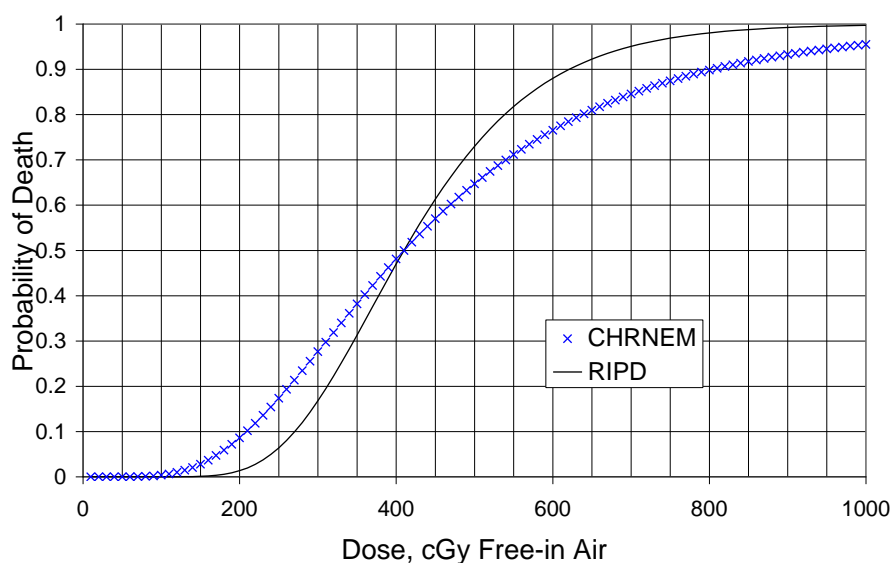


**Figure 1. The prompt dose mortality curve used in RIPD has a steeper slope than that of the older CHRNEM software.**

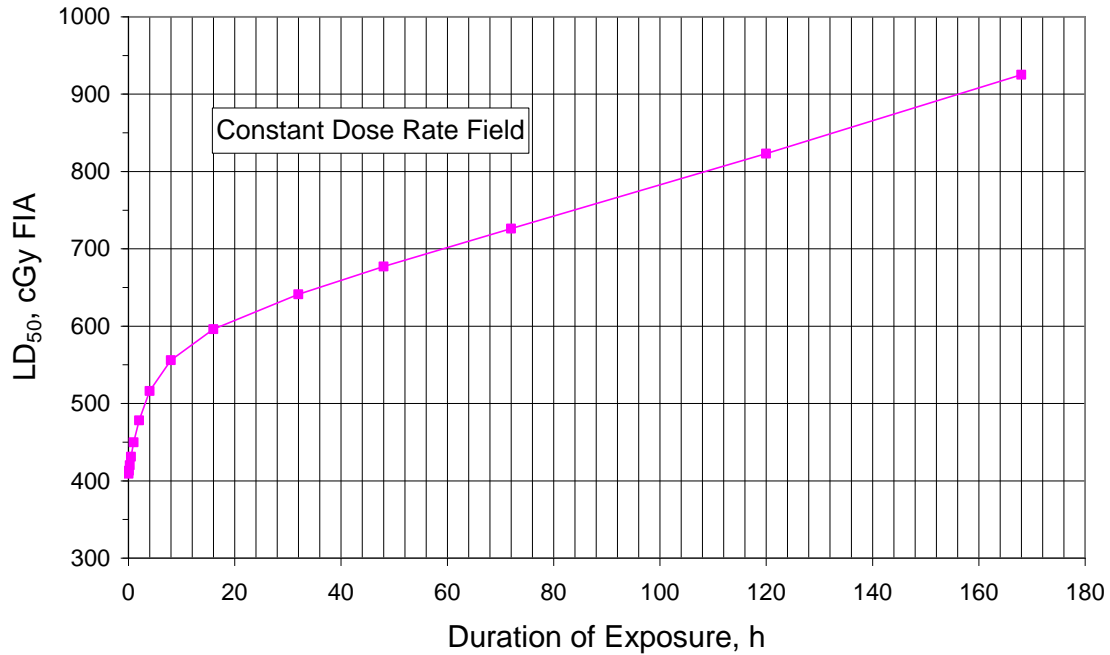
## **Section 4.**

### **Exposure at Constant Dose Rate**

One way to characterize a protracted exposure to ionizing radiation is by specifying two parameters: a (constant) dose rate and an exposure duration. Given values for these parameters, one can calculate integrated dose and estimate biological effect. In this section we describe how the MARCELL model relates integrated dose to biological effect, for the case of constant dose rate exposures.

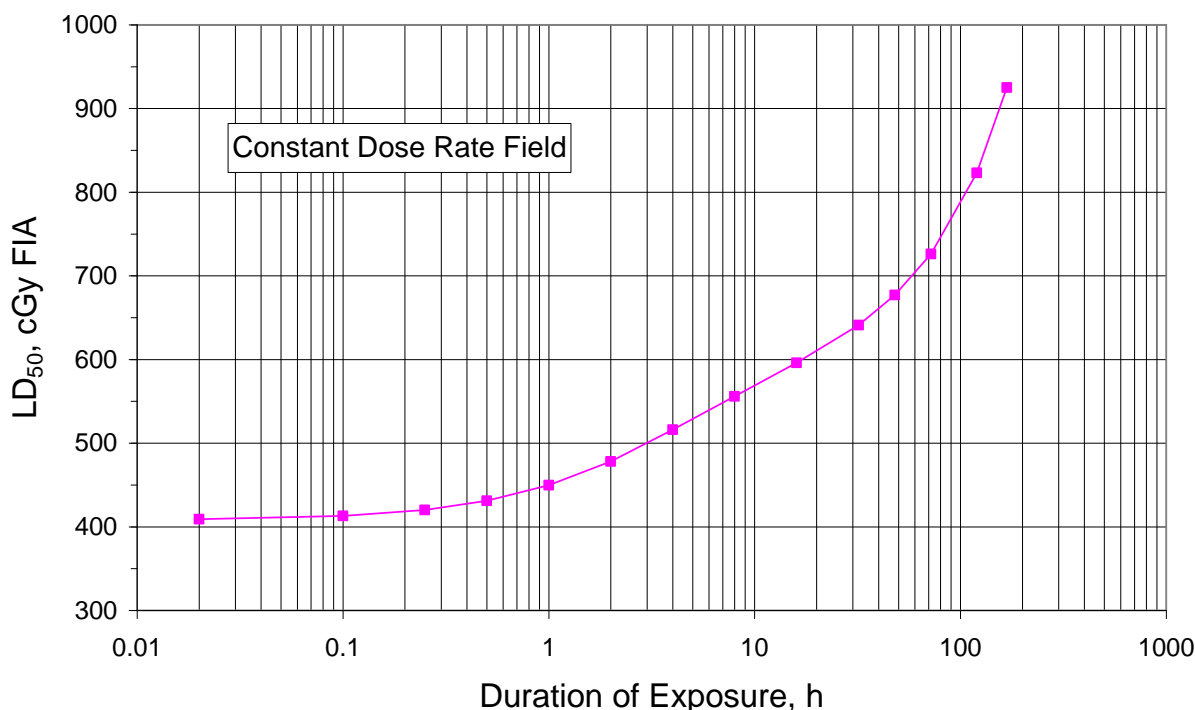
For an individual in a constant dose rate field of moderate duration, the marrow cell population calculated from the MARCELL model falls monotonically, approaching a limiting population level that depends on the magnitude of the dose rate. At the end of the radiation exposure, the cell population begins a recovery to its normal equilibrium value. The resulting cell population nadir occurs at the end of the exposure when radiation damage ceases and repair processes continue. For a fixed total dose, increasing the exposure duration lowers the dose rate during exposure, resulting in less depletion of the cell population at the nadir. Therefore, the median lethal dose ( $LD_{50}$ ) is larger for longer exposures. Figure 2 plots data from RIPD v2.0 showing the dependence of  $LD_{50}$  on the duration of exposure for exposures at constant dose rate. In the limit of zero duration of exposure, the  $LD_{50}$  equals 410 cGy, the value for a prompt exposure.

Note that in Figure 2 there is a different “constant” dose rate for each duration of exposure. The plot is a contour curve in the sense of biological effect: each point on the curve represents an exposure (a dose rate, exposure duration pair) that results in a 50% probability of mortality. Note that, by fixing biological effect, dose rate is a function of exposure duration, so only one parameter, exposure duration, is needed to specify the exposure scenario.



**Figure 2. Because of biological repair and recovery processes, the median lethal dose for exposures at a constant dose rate increases with increasing duration of exposure.**

There are characteristic time constants associated with the physiological processes modeled in MARCELL. These characteristic times are associated with cell proliferation and the repair of radiation damage. Together they determine the shape of the curve in Figure 2. To display the effects of these characteristics times more clearly, Figure 3 shows the data of Figure 2 plotted on a logarithmic time scale. Below about 10 minutes, the dependence on exposure duration is weak; the LD<sub>50</sub> differs little from that for a prompt exposure. For exposures longer than half an hour, the LD<sub>50</sub> begins to rise significantly. For exposure durations between about one hour and 30 hours, the curve in Figure 3 is nearly straight, indicating an approximate power law dependence of LD<sub>50</sub> on duration of exposure. For exposure durations longer than about 50 hours (or 2 days), the curve turns up more steeply.



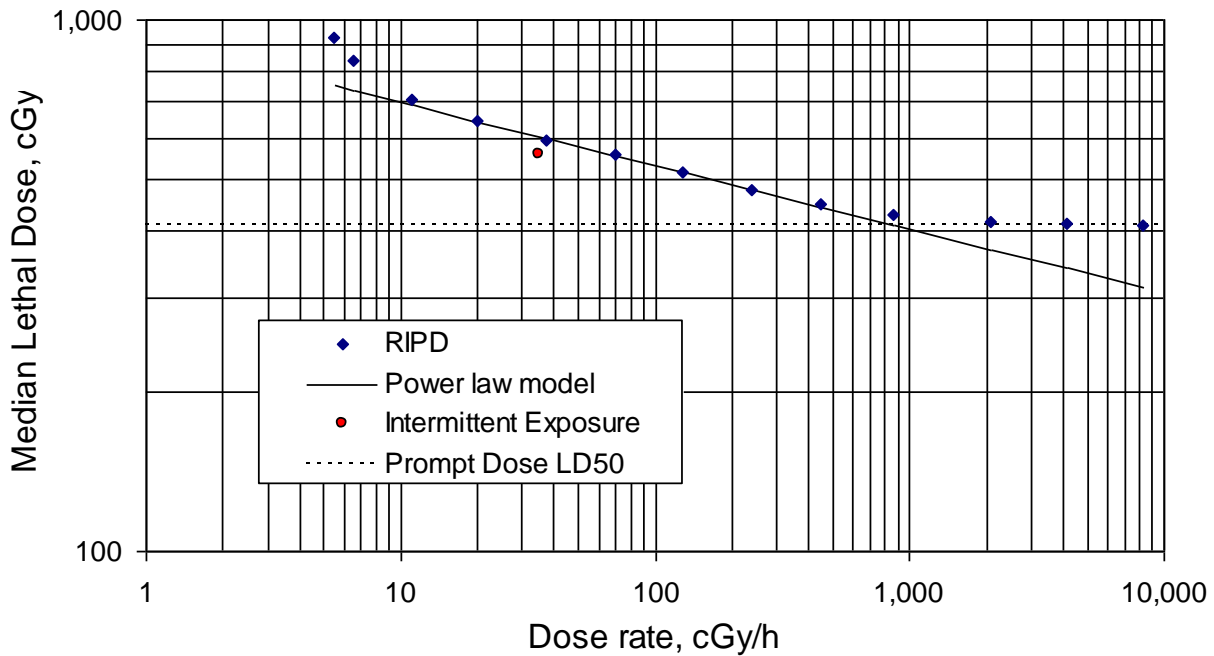
**Figure 3. Data from Figure 2 plotted with a logarithmic time scale.**

Figure 4 plots similar LD<sub>50</sub> data calculated with RIPD v2.0 showing the LD<sub>50</sub> for constant dose rate exposures as a function of dose rate rather than exposure duration. The straight solid line representing power law behavior is a regression fit to the five data points between dose rates of 20 and 300 cGy/h. In log-log space (base 10), the slope and intercept of the straight line are 2.9634 and -0.11918, respectively.

Figure 4 illustrates a principle having wide application in the theory and analysis of human response data, namely, that power law models are useful but extreme caution is required regarding extrapolation. It is common to use a power law model to analyze and describe experimental toxicity data when a suitable physiologically based model of response (either human or animal) is not available. Because experiments are costly, there is rarely enough data to map out the full range of response in terms of exposure rate or duration. Frequently, the data in the range of experimentation can be described quite well by a power law relationship between response and exposure rate or duration. Such is the case for the toxic load model of the effects of chemical exposure. Modelers must keep in mind that these power law relationships can rarely be extrapolated with confidence to either long or short duration exposures (low or high dose rates). Figure 4 illustrates this point for a physiologically based model of the response to ionizing radiation exposure. The power law works quite well in a limited range of dose rates but fails to extrapolate correctly to either low or high dose rates.

The single data point labeled “Intermittent Exposure” in Figure 4 is the RIPD calculation of the LD<sub>50</sub> for four equal doses of 1 h duration starting at 0, 5, 10, and 15 h, respectively, for a total exposure period 16 h. The LD<sub>50</sub> for this fractionated exposure is 559 cGy or an average dose rate of 35 cGy/h during the 16 h period. The solid line in Figure 4 shows that the LD<sub>50</sub> for a constant dose rate of 35 cGy/h is just over 600 cGy. From Figure 3, the LD<sub>50</sub> for a single one hour

exposure is about 450 cGy. Therefore, the effect of fractionation on the  $LD_{50}$  is intermediate between that of a one hour exposure (corresponding to the length of individual fractions) and a sixteen hour exposure (corresponding to the total exposure period). The effect is closer to that of a sixteen hour exposure. The total time during which the exposure is non-zero for the fractionated exposure is four hours. From Figure 3, the  $LD_{50}$  for a four-hour exposure is about 520 cGy, so the effect of the fractionated exposure is midway between that for the four-hour and the 16-hour exposure periods. That is, the effect is midway between that of an exposure with the duration of the fractionated exposure's non-zero exposure rate and that of an exposure with duration equal to the fractionated exposure's total duration.



**Figure 4. Median lethal dose for exposures at constant dose rate plotted as a function of dose rate (exposure duration is determined by dose rate, because biological effect is fixed).**

Figure 5 examines the behavior of the MARCELL model from the viewpoint of a fixed total dose of 410 cGy delivered at different fixed dose rates (*i.e.*, different exposure durations). Figure 5 shows that the equivalent prompt dose for mortality approaches 410 cGy at high dose rates as it must to be biologically reasonable. At low dose rates, the EPD decreases rapidly, consistent with the fact that dose rates approaching natural background will have negligible effect on mortality. In the intermediate range between 10 and 1000 cGy/h, the dependence of EPD on dose rate is well described by a power law. The regression fit to the six points between 10 and 500 cGy/h results in an intercept and slope of 2.3494 and 0.085302, respectively, in log-log space (base 10). The single point labeled “Intermittent Exposure” is for the same fractionated schedule as that in Figure 4 with a dose rate of 102.5 cGy/h during each pulse and an average of 25.63 cGy/h for the 16 hour period of exposure.



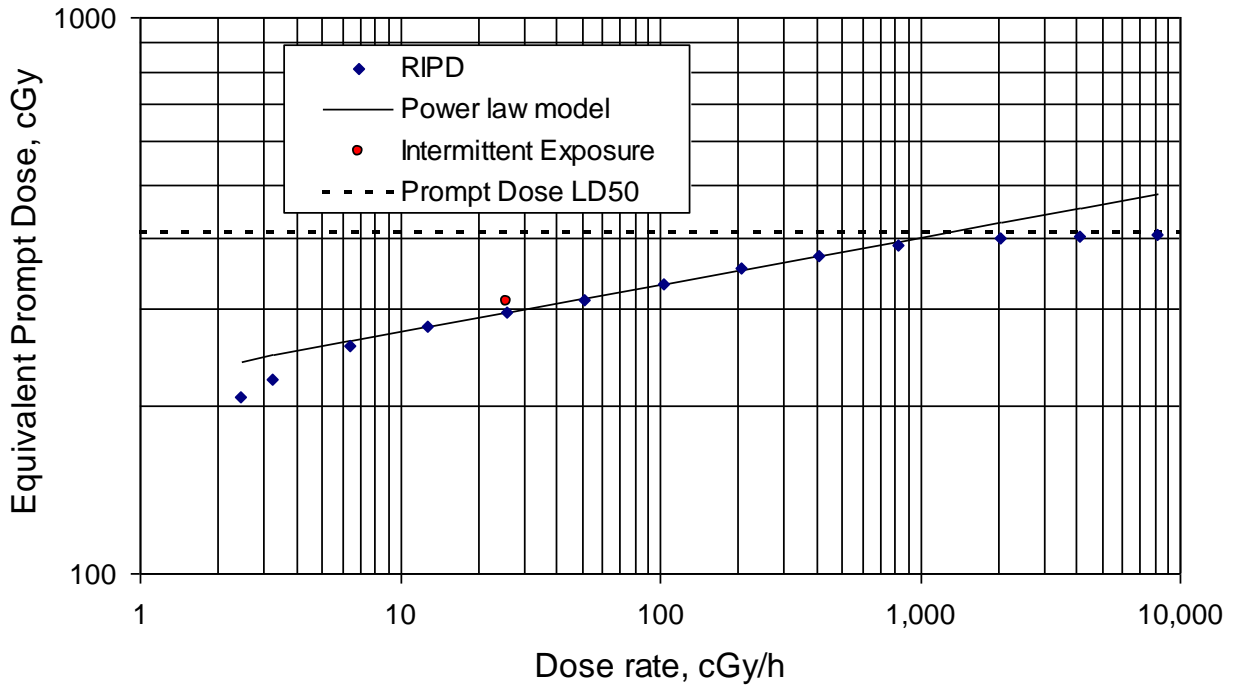


**Figure 5. The EPD for a 410 cGy dose delivered at constant dose rate also has a power behavior over a limited range of dose rates.**

## Section 5.

### Dose-Response Approximations for Exposure at Constant Dose Rate

This section presents two methods for approximating the lethal effects of exposure at constant dose rate described in the previous section. It is useful to have information on the shape of the dose response curve as well as the median lethal dose. In this regard, Figure 6 plots as a function of duration of exposure the 10% and 90% lethal doses ( $LD_{10}$  and  $LD_{90}$ , respectively) for exposures at constant dose rate as well as the  $LD_{50}$  described previously.

Table 1 lists the data plotted in Figure 6 as well as the ratio of  $LD_{90}$  to  $LD_{10}$ , which is determined by the slope of the dose response curve. The relatively small variation of this ratio over the more than three orders of magnitude change in duration of exposure indicates that variation of the slope might be neglected in constructing a simple model of the effect of dose protraction on the dose-response curve for mortality. The ratio changes by only 13% while the  $LD_{50}$  increases by 65% over this range.

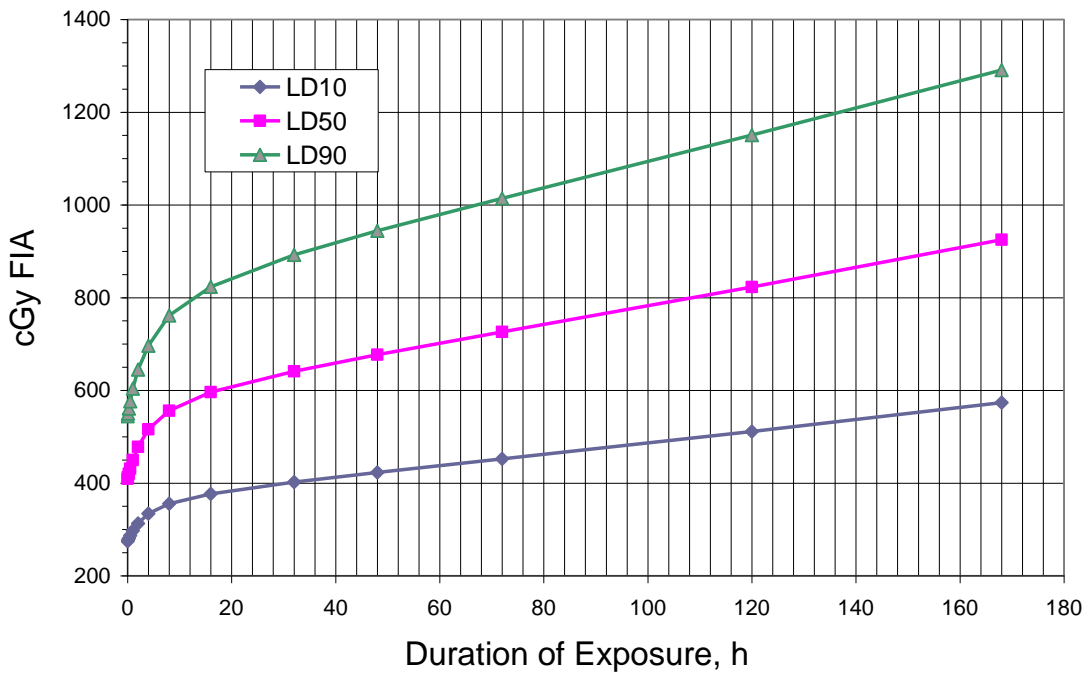


**Figure 6. Response parameters for constant dose rate exposure.**

**Table 1. Data from Figure 6 showing the relatively small variation in the slope of the dose response curve as measured by the ratio of the LD<sub>90</sub> to the LD<sub>10</sub>.**

<i>Exposure Duration</i>	<i>LD<sub>10</sub></i>	<i>LD<sub>50</sub></i>	<i>LD<sub>90</sub></i>	<i>LD<sub>90</sub>/LD<sub>10</sub></i>
<i>h</i>	<i>cGy</i>	<i>cGy</i>	<i>cGy</i>	
0.02	274.7	409.5	544.3	1.98
0.1	276.9	413.4	550.1	1.99
0.25	280.9	420.4	560.6	2.00
0.5	286.9	431.2	576.6	2.01
1	297.3	449.7	603.9	2.03
2	312.8	477.6	644.9	2.06
4	334.2	516.0	696.2	2.08
8	355.5	555.7	761.4	2.14
16	376.9	595.8	823.2	2.18
32	402.1	641.5	892.3	2.22
48	422.7	677.0	944.1	2.23
72	452.0	726.0	1014.2	2.24
120	511.1	823.3	1150.5	2.25
168	573.4	924.7	1291.1	2.25

Radiological weapons (“dirty bombs”) will in most cases disperse radionuclides whose half-life is long enough that the dose rate in contaminated areas will be essentially constant over most emergency response scenarios. Therefore the data presented here is directly applicable to resulting whole-body gamma ray exposures. For a quick estimate of the median lethal dose ( or the LD<sub>90</sub> or LD<sub>10</sub>) for a given scenario, one may simply use Table 1 as a look-up table, interpolating relative to exposure duration if desired. Alternatively, the data in Table 1 may be fitted with an analytic curve to provide an estimate at any exposure duration within the given range of durations. We tested several alternatives and found that a sixth-order polynomial relating  $y = \log_{10}(\text{dose in cGy})$  to  $x = \log_{10}(\text{time in hours})$  gave a good compromise between simplicity and accuracy. Therefore, we have the expression

$$y = \sum_{n=0}^6 c_n x^n . \quad (1)$$

The coefficients  $c_n$  for the three sets of data shown in Figure 6 are listed in Table 2. The smooth curves in Figure 6 are generated by the Microsoft Excel plotting utility. Curves generated by Equation 1 with the coefficients from Table 2 are plotted for LD<sub>50</sub>, LD<sub>10</sub>, and LD<sub>90</sub> in Figure 7, Figure 8, and Figure 9, respectively. Equation 1 may be used between 0.1 and 168 h.

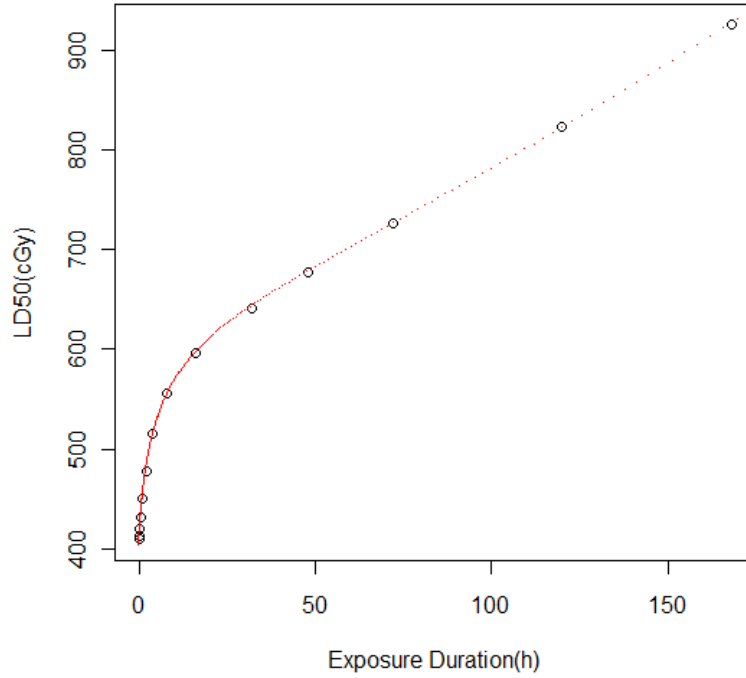


**Figure 7. Curve shows sixth-order polynomial fit to the  $LD_{50}$  data (circles) from Table 1. Coefficients of the polynomial are listed in Table 2.**

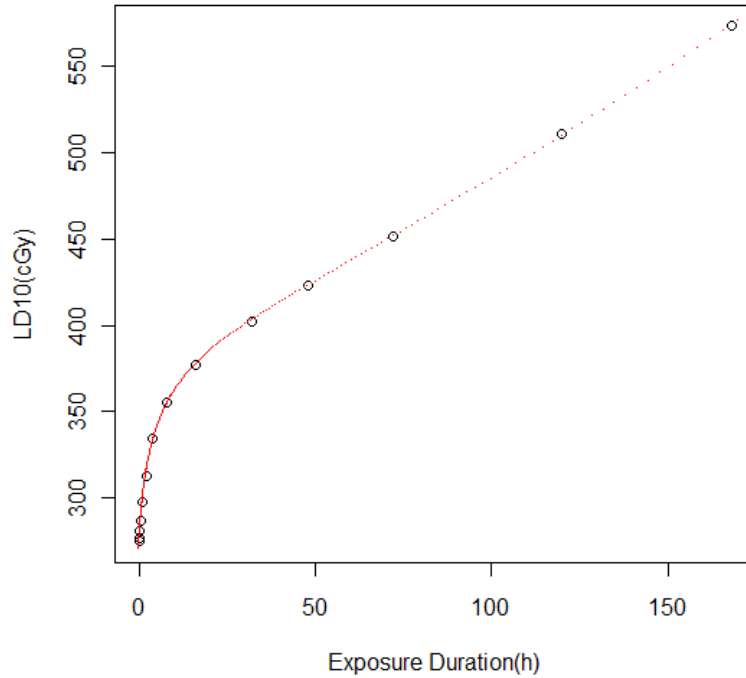


**Figure 8. Curve shows sixth-order polynomial fit to the  $LD_{10}$  data (circles) from Table 1. Coefficients of the polynomial are listed in Table 2.**

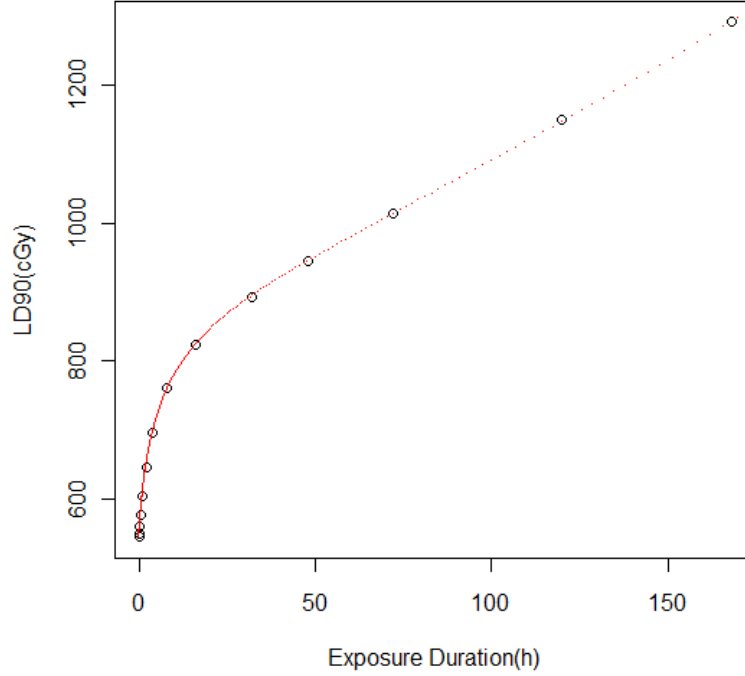


**Figure 9. Curve shows sixth-order polynomial fit to the  $LD_{90}$  data (circles) from Table 1. Coefficients of the polynomial are listed in Table 2.**

**Table 2. Coefficients for sixth-order polynomial fits to the data in Table 1. Independent variable is  $\log_{10}(\text{time in hours})$ . Polynomial gives  $\log_{10}(\text{dose in cGy})$ .**

<i>Coefficient:</i>	$c_0$	$c_1$	$c_2$	$c_3$	$c_4$	$c_5$	$c_6$
$LD_{90}$	2.781	0.08238	0.04383	-0.008851	-0.01075	0.001748	0.001609
$LD_{50}$	2.654	0.07762	0.03944	-0.01164	-0.009152	0.002541	0.001309
$LD_{10}$	2.474	0.06620	0.03308	-0.01106	-0.007633	0.002600	0.001161

The  $LD_{50}$  data in Table 1 has also been fit as a function of dose rate (Oxford, 2016), using the following formula:

$$LD_{50}(DR) = \frac{LD_{50}(0.02)}{c_0 \cdot c_1^{DR} \cdot DR^{c_2} + c_3}. \quad (2)$$

Where  $LD_{50}(DR)$  is the value of the  $LD_{50}$  (in Gy) at dose rate  $DR$  (in Gy/h). The coefficients for this fit are given in Table 3, below.

This functional form was derived using open-source curve-fitting software which is available at the website <https://github.com/zunzun/pyeq2>. This software fits a large number of linear and non-linear functions to a given data set, using a genetic algorithm to find initial values for the fits. It then ranks the fits, using a measure such as Akaike Information Criteria (AIC), and reports these results back to the user. The form of Equation 2 was selected from the top three

ranked functions returned by the software, and was the only function which gave reasonable values when extrapolating outside the dose rate range of the fitted data (Oxford, 2016).

**Table 3: Coefficients for fits of function given in Equation 2 to  $LD_{50}$  data given in Table 1. Independent variable is dose rate in Gy/h. Equation 2 gives the value of  $LD_{50}$  in Gy.**

<i>Coefficient:</i>	$c_0$	$c_1$	$c_2$	$c_3$
$LD_{50}$	-0.2351	0.8946	-0.2876	-0.9947

$LD_{50}$  as a function of dose rate from the data in Table 1 and from the fit given by Equation 2 is shown in Figure 10.

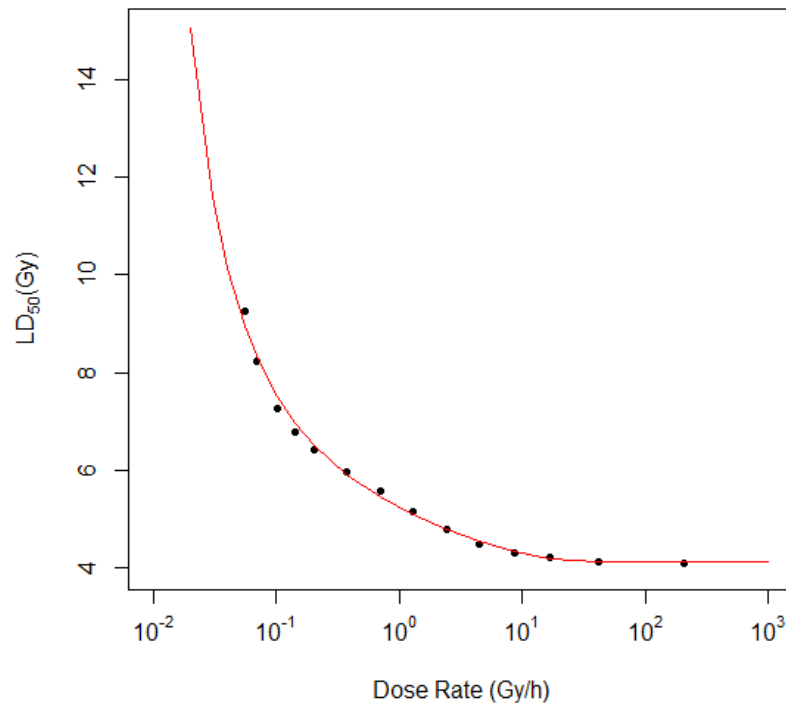


**Figure 10: Curve shows Equation 2 fitted to the  $LD_{50}$  values (circles) from Table 1. Coefficients for Equation 2 are given in Table 3.**

## Section 6.

### Exposure in a Nuclear Fallout Field

At minimum, one extra parameter is needed to characterize exposure to a nuclear fallout field. For a constant dose rate exposure, the two independent variables describing the exposure are the dose rate and the exposure duration. For a fallout exposure, the corresponding variables are the dose rate at entry into the fallout field and the exposure duration; however, an additional independent variable is needed to specify the rate of decrease of the dose rate, that is, the dose rate decay. Because the decay of the various radionuclides begins at the time of nuclear detonation and because short-lived radionuclides become negligible quickly, the rate of decrease of the dose rate during the exposure period depends strongly on the age of the fallout at the time of entry. The average radionuclide decay rate is much faster soon after the detonation than it is later. Therefore, the age of the fallout at the time of entry is needed as a third independent variable to fully specify the dose rate history for a fallout exposure.

Over the range of time-after-detonation and exposure durations considered in this paper, the decay of radionuclides gives a dose rate history that is well approximated by a power law as a function of time. Commonly, the dose rate decay has been approximated by the function  $t^{-1.2}$ . More recently, (as in HPAC v4.x), the curve is being approximated with  $t^{-1.3}$ . RIPDLIPI in HPAC 4.x is based on RIPD calculations with  $t^{-1.3}$ . The calculations illustrated in this paper are based on Version 2.1 of RIPD, which used  $t^{-1.2}$ . The features of human response to fallout field exposure described in this paper are not significantly affected by this small difference in exponent.

Operationally, two factors will determine the fallout age-at-entry. The first, obviously, is the time of personnel movement into the fallout field either from a remote location or from a fallout shelter. This movement may occur soon after fallout deposition or many months later. The second factor is the atmospheric transit time from the point of detonation to the location of interest. The transit time consists of the time needed for the radionuclides to rise with the nuclear fireball, drift downwind, and fall to the ground at the location of exposure. This atmospheric transit time places a lower limit on the fallout age at the beginning of exposure. It depends on both meteorology and weapon yield. For kiloton yields it may be as small as a few minutes but for megaton yields several hours or longer depending on range downwind. Because of spatial dispersion of the nuclear cloud during atmospheric transit, the deposition of fallout is not instantaneous but rather occurs over a period of time during which the dose rate rises to a maximum at a given location. For present purposes, this deposition time is assumed to be short compared to the duration of exposure and is neglected.

Because three independent variables are needed to specify the dose rate dependence during exposure to a fallout field rather than the two needed for exposure at constant dose rate, it is convenient for comparisons to fix one of the three variables for the fallout exposure. Figure 11 shows such a comparison fixing the age-at-entry equal to one hour for the fallout exposure. Figure 11 plots RIPD (MARCELL) predictions for LD<sub>50</sub> as a function of duration of exposure (given age-at-entry equal to one hour, the remaining exposure parameter, dose rate at entry, is determined by duration of exposure). There is little difference between the fallout and constant

dose rate curves for duration of exposure less than 100 hours. For longer durations, the constant duration exposure is less damaging ( $LD_{50}$  is higher) because it does not have the high dose rate peak at early times characteristic of fallout exposure. (Similar to Figure 2, Figure 11 is a contour curve in the sense of biological effect: each point on the curve represents an exposure (i.e., specified values of fallout age at entry, exposure duration, and dose rate at entry) that results in a 50% probability of mortality. By fixing biological effect and fallout age at entry, dose rate at entry is a function of exposure duration, so only one parameter, exposure duration, is needed to specify the exposure scenario).

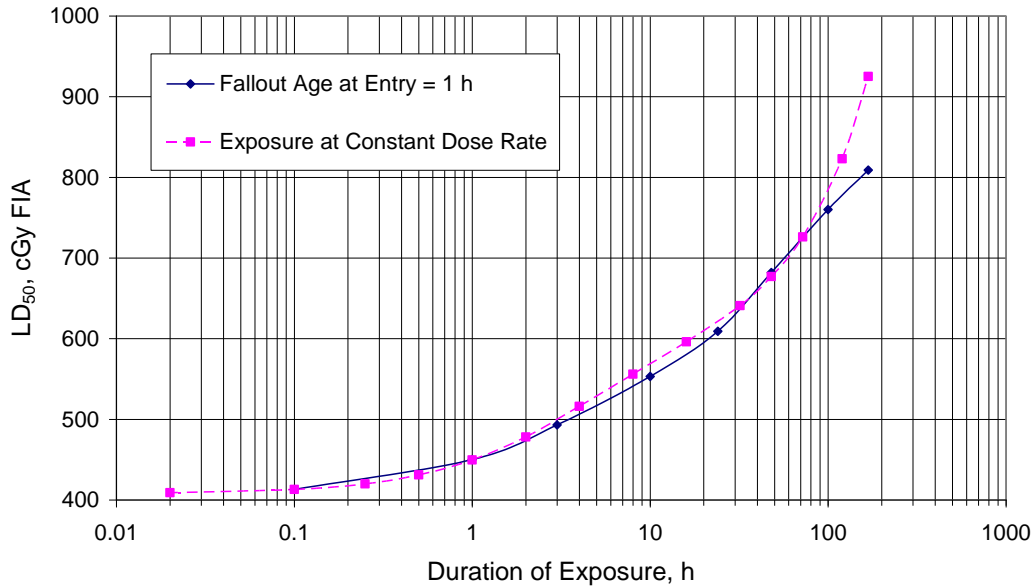


**Figure 11. With fallout age fixed at 1 h, the median lethal dose as a function of exposure duration is similar to that for a constant dose rate exposure when the exposure duration is less than four days.**

Figure 12 shows the  $LD_{50}$  as a function of fallout age-at-entry for exposure duration fixed at 48 hours. As the age-at-entry increases, the dose rate during the exposure becomes flatter, and will eventually approach a constant during the fixed 48 hour period. Figure 2 shows that the  $LD_{50}$  for a constant dose rate exposure is about 680 cGy so, as expected, the curve in Figure 12 levels out at about that value for increasing fallout age-at-entry. As age-at-entry decreases, the dose rate becomes quite peaked at the beginning of exposure, leading to an  $LD_{50}$  tending toward the prompt dose value as shown in Figure 12.



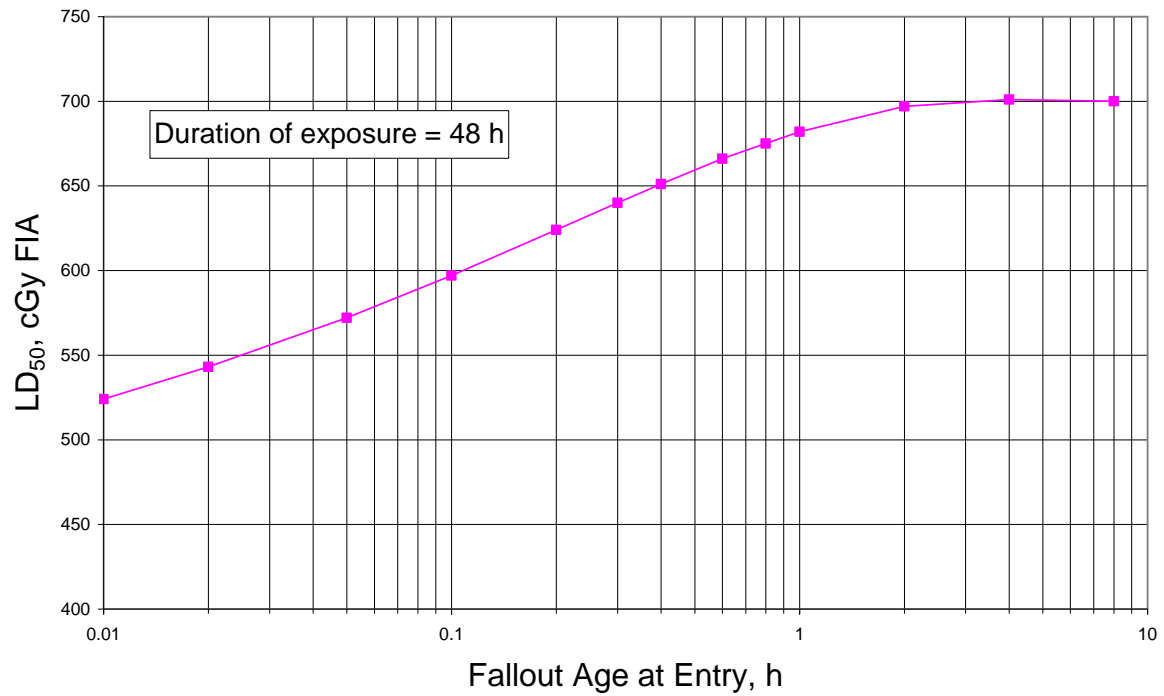


**Figure 12.** The median lethal dose for a 48 h exposure in a fallout field depends on the age of the fallout at the time of entry into the fallout field.

## Section 7.

### Dose-Response Approximation for Exposure in a Fallout Field

To provide a first approximation for the probability of mortality due to a single exposure period in the fallout field of a nuclear detonation, we can estimate the  $LD_{50}$  and probit slope for the dose response curve for such an exposure using information presented in the two previous sections. Our method consists of using the approximation for exposure at constant dose rate and making a correction for the effect of the decay of the dose rate over time. Although this correction actually varies somewhat with age of fallout, we use a single correction independent of age that gives a good approximation for ages of operational interest for those in the open downwind of a surface burst in the aftermath of a surface or near surface detonation.

Because of cloud stabilization time and deposition time of the fallout, most fallout exposures at ground level (away from the base surge) will begin at fallout ages of at least 10 to 20 minutes. In that case, Figure 12 shows that the  $LD_{50}$  will be closer to that of a constant dose rate exposure than a prompt dose. As an approximation to the  $LD_{50}$ , we can use a weighted average of the prompt dose value and the constant dose rate value for the exposure duration of interest. Focusing on the data for a 48-h duration of exposure and a fallout age at entry of 0.3 h (*i.e.*, 18 min.), we find that weighting the constant dose rate value six times heavier than the prompt dose value provides a good estimate. The formula for the weighted  $LD_{50}$  as a function of duration of exposure is then:

$$weightedLD_{50}(duration) = \frac{LD_{50}prompt + 6 \times LD_{50}const(duration)}{7}. \quad (3)$$

This “rule of thumb” formula yields a value of 639 cGy for the weighted  $LD_{50}$  in good agreement with RIPD calculations as illustrated in Figure 13.

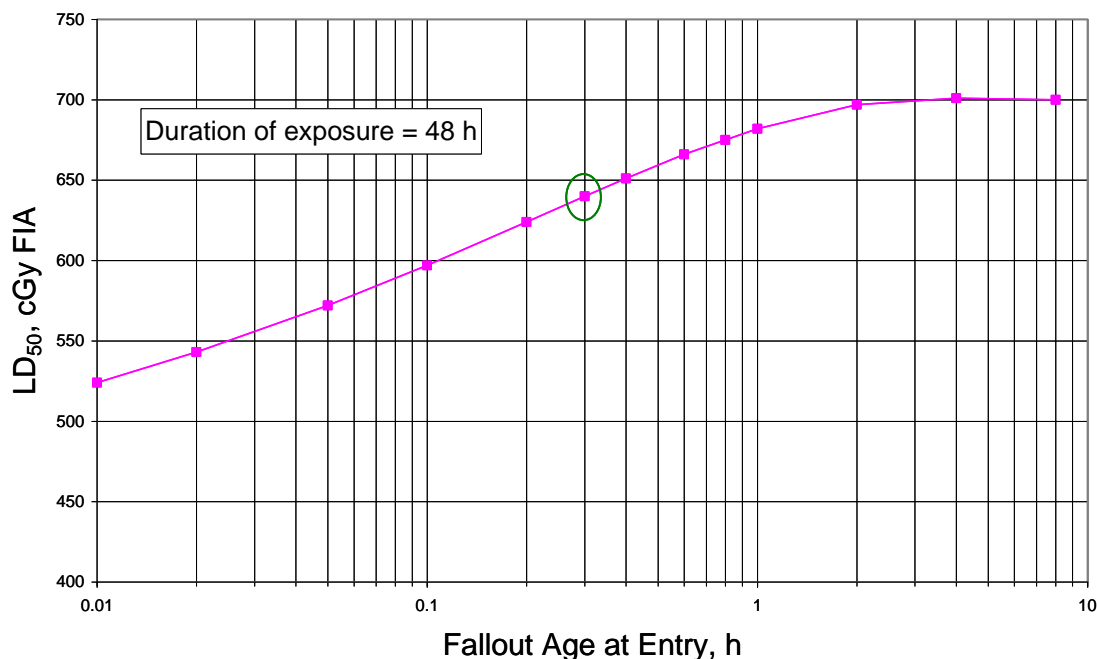


**Figure 13. The rule of thumb gives an LD<sub>50</sub> of about 640 cGy (circled point) for a 48 h exposure, in quite good agreement with the fallout calculation from RIPD for a fallout age at entry of 0.3 h.**

To illustrate the effect of neglecting fallout age in the rule of thumb, Table 4 compares weighted values of LD<sub>50</sub> given by the rule of thumb with RIPD calculations for 0.2 h and 1.0 h ages at entry. The comparison shows that the rule of thumb values reflect the RIPD values quite closely for fallout age at entry of 10 to 20 minutes. The rule of thumb underestimates the LD<sub>50</sub> somewhat for age at entry of 1 h. This underestimate of the LD<sub>50</sub> provides a defense-conservative estimate of casualties.

**Table 4. Rule of thumb provides results intermediate to fallout ages of 0.2 and 1.0 h.**

Exposure Duration h	LD50 (Free-In-Air, whole-body gamma)			
	Steady Exposure cGy	Fallout Age 0.2 h	Rule of Thumb	Fallout Age 1.0 h
		(RIPD) cGy		(RIPD) cGy
2	478	468	468	476
4	516	491	501	506
24	618	578	588	609
48	677	624	639	683

In summary, an approximate method for estimating the probability of mortality due to fallout exposure in the aftermath of a nuclear detonation accounting for dose protraction is the following:

1. Choose a fallout exposure duration appropriate to the desired scenario, but not exceeding 4 days nor less than 0.1 h.
2. Determine the  $LD_{50}$  for an exposure of that duration at constant dose rate (use Table 1 or Equation 1).
3. For early fallout exposure (*i.e.*, beginning 0.2 to 1 h after detonation), use Equation 3 to estimate the  $LD_{50}$ .
4. For later exposures (starting several hours after detonation), use the constant dose rate value from Step 2 for the  $LD_{50}$ .
5. Use the same value of the probit slope as for prompt doses (see Section 3).

For radiological scenarios, an approximate method is the following:

1. Choose an exposure duration appropriate to the desired scenario, but in the range for 0.1 h to 168 h.
2. Determine the  $LD_{50}$  for an exposure of that duration at constant dose rate (use Table 1 or Equation 1).
3. Use the same value of the probit slope as for prompt doses (see Section 3).

## Section 8.

### Conclusion

Aside from continuing improvement of documentation of models in HPAC, a primary motivation for this paper is to better understand why the Probability of Fatality plots in HPAC for exposure to nuclear weapon fallout so frequently indicate median lethal doses in the vicinity of 700 cGy rather than the prompt dose value of 410 cGy as illustrated in Figure 14. This result has seemed counter-intuitive to some. However, the analysis presented in this paper shows that such values are quite reasonable in the context of the MARCELL model. It seems that typical values of fallout age-at-entry and exposure duration encountered in HPAC calculations tend to generate protracted exposures having LD<sub>50</sub> ranging from 600 to 700 cGy.

As a byproduct of this analysis, we present approximate methods for estimating the probability of mortality due to radiological environments from nuclear weapon detonations or from a radiological dispersal device.

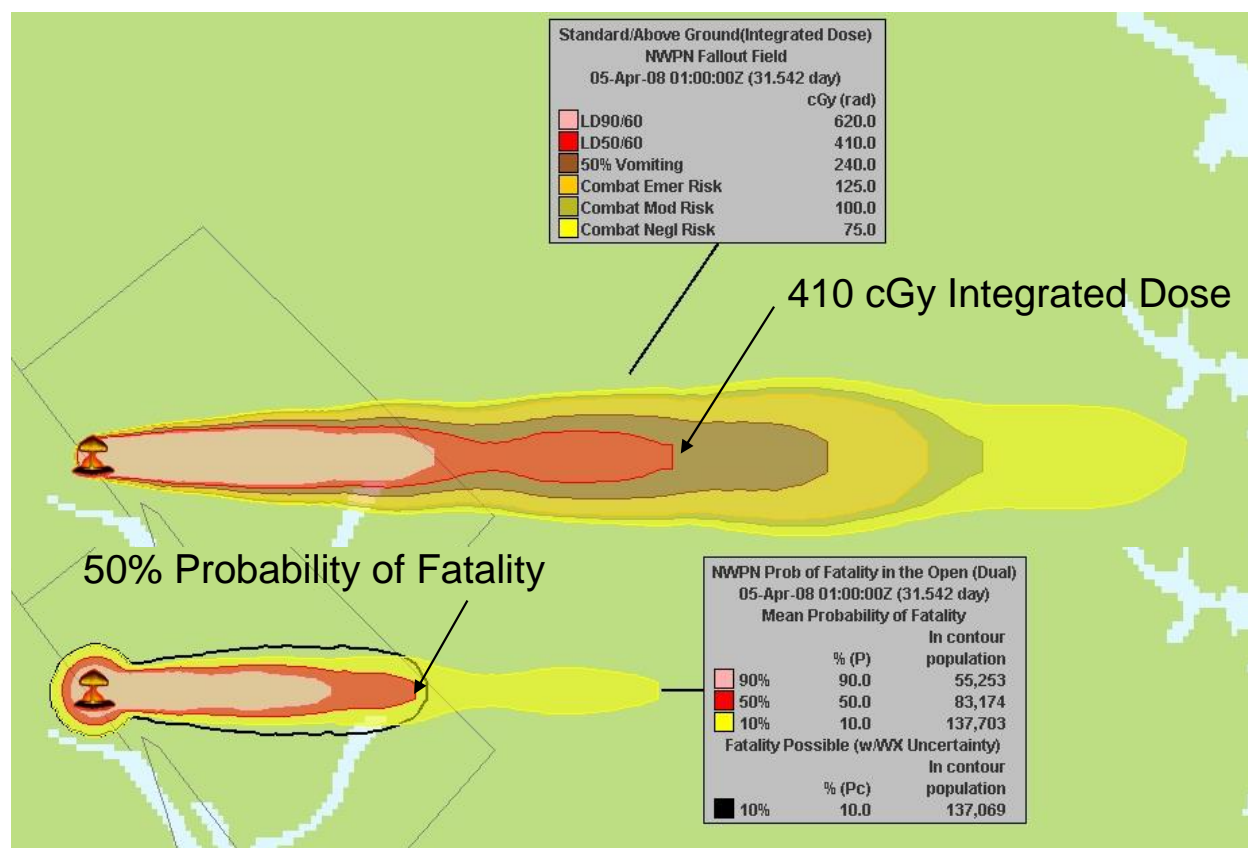


**Figure 14. HPAC comparison of 48-hour integrated dose from fallout and the resulting probability of fatality shows the reduction in mortality caused by dose protraction for a 10 KT ground burst. (Note that the probability of fatality includes prompt weapon effects while the integrated dose does not.)**

## Section 9.

### References

- Anno, G. H., G. E. McClellan, M. A. Dore, and S. J. Baum, "Biological Effects of Protracted Exposure to Ionizing Radiation: Review, Analysis, and Model Development," DNA-TR-90-157, Defense Nuclear Agency, Alexandria, Virginia 22310-3398, November 1991.
- Anno, G. H., G. E. McClellan, and M. A. Dore, "Protracted Radiation-Induced Performance Decrement, Volume 1 – Model Development," DNA-TR-95-117-V1, Defense Nuclear Agency, Alexandria, Virginia 22310-3398, May 1996.
- Anno, G. H. et al., "Dose Response Relationships for Acute Ionizing-Radiation Lethality," *Health Phys.* 84, 5:565, 2003.
- Jones, T.D., M.D. Morris, and R.W. Young, "A Mathematical Model for Radiation-Induced Myelopoiesis," *Radiation Research* 128: 258-266, 1991.
- Jones, T.D., M.D. and Morris, and R.W. Young, "Mathematical Models of Marrow Cell Kinetics: Differential Effects of Protracted irradiations on Stromal and Stem Cells in Mice," *Int. J Radiat. Oncol. Biol. Phys.* 26: 817-830, 1993a.
- Jones, T.D., M.D. Morris, and R.W. Young, Kehlet, R.A., "A cell-kinetics model for radiation induced myelopoiesis," *Experimental Hematology* 21: 816-822, 1993b.
- Jones, T. D., M. D. Morris, and R. W. Young, "Dose-Rate RBE Factors for Photons: Hematopoietic Syndrome in Humans vs. Stromal Cell Cytopenia," *Health Phys.* 67:495-508; 1994a.
- Jones, T.D., M.D. Morris, and R.W. Young, "Do stem or stromal cells control hematopoietic recovery after irradiation?," *Experimental Hematology* 22: 3-4, 1994b.
- Jones, T.D., Morris, M.D., R.W. Young, and R.A. Kehlet, "Neutron RBEs for Cytopenia and Repopulation of Stroma and Hematopoietic Stem Cells: Mathematical Models of Marrow Cell Kinetics," *Health Physics* 72(4): 530-543, 1997.
- Levin, S.G., and J. W. Fulton *Consolidated Human Response Nuclear Effects Model (CHRNEM)*, Technical Report, DNA-TR-93-45, Defense Nuclear Agency, Alexandria, VA, September 1992
- Matheson, L. N., M. A. Dore, G. H. Anno, and G. E. McClellan, "User's Manual: Radiation-Induced Performance Decrement (RIPD) – Version 2.0," DNA-TR-95-91, Defense Nuclear Agency, Alexandria, Virginia 22310-3398, 1996.
- Matheson, L. N. and G. E. McClellan, " HPAC Effects Module RIPDLIPI: Radiation-Induced Performance Decrement (RIPD) Lethality Injury Probability Interpolation," HPAC V&V Report, Defense Threat Reduction Agency, Alexandria, Virginia 22310-3398, June 30, 2004.
- Morris, M.D., T.D. Jones, and R.W. Young, "Estimation of Coefficients in a Model of Radiation Induced Myelopoiesis from Mortality Data for Mice following X Ray Exposure," *Radiation Research* 128: 267-275, 1991.

Morris, M.D., T.D. Jones, and R.W. Young, “Bone marrow equivalent prompt dose from two common fallout scenarios,” *Health Physics* 67: 183-186, 1994.

Oxford, S. *Private communication*, Institute for Defense Analyses, 2016.